MODELING OF DIPOLE AND QUADRUPOLE FRINGE-FIELD EFFECTS FOR THE ADVANCED PHOTON SOURCE UPGRADE LATTICE *

M. Borland, R. Lindberg, ANL, Argonne, IL 60439, USA

Abstract

The proposed upgrade of the Advanced Photon Source (APS) to a multibend-achromat lattice requires shorter and much stronger quadrupole magnets than are present in the existing ring. This results in longitudinal gradient profiles that differ significantly from a hard-edge model. Additionally, the lattice assumes the use of five-segment longitudinal gradient dipoles. Under these circumstances, the effects of fringe fields and detailed field distributions are of interest. We evaluated the effect of soft-edge fringe fields on the linear optics and chromaticity, finding that compensation for these effects is readily accomplished. In addition, we evaluated the reliability of standard methods of simulating hard-edge nonlinear fringe effects in quadrupoles.

INTRODUCTION

The APS Upgrade (APS-U) project plans to replace the existing 3rd-generation storage ring with a multi-bend achromat (MBA) design [1] that will reduce the emittance to less than 70 pm [2,3]. The goal is to replace the existing storage ring and return to user operation within 12 months. One important factor in achieving this will be thorough understanding of the lattice and beam dynamics with realistic models of the magnets. This paper reports progress on this issue with respect to modeling of quadrupole and dipole magnets.

The integrated quadrupole strength for low-emittance lattices scales like N_d, where N_d is the number of dipoles per sector [4]. One strategy for dealing with this is to use smaller magnet apertures, which may impact field quality. Magnets may also be operated in a more highly-saturated condition. The latter condition in particular will increase the difficulty of modeling linear and nonlinear edge effects.

The APS-U lattice includes several types of dipole magnets, including two types of 5-segment longitudinal gradient dipoles. The former are quite unfamiliar and hence merit close attention. Of interest is ensuring that the trajectory through the magnets is correct, assessing the effect on linear optics, and understanding the impact on chromaticity and other nonlinear properties.

QUADRUPOLE MODELING

The initial design of the APS-U quadrupoles made use of "mushroom" pole tips, which extend under the coils in order to increase the effective length of the magnets. This allowed operating with higher magnetic efficiency for a given integrated gradient, without unduly increasing the magnet core length. It also allowed making most magnets of identical lengths, with nearly identical cores and coils. However, the resulting gradient profile shape depended strongly on the level of excitation as shown in Fig. 1. With the exception of the 98% efficiency case, corresponding to an integrated gradient of ~12 T, the profiles are very unusual.

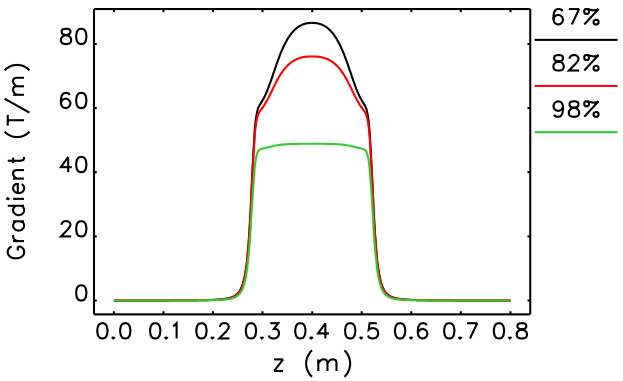

Figure 1: Gradient profiles for initial APS-U quadrupoles at various levels of magnetic efficiency.

Our first task was to assess the impact of such profiles on beam transport. This was done using the approach described in [5,6] for modeling soft-edge effects. For the hard-edge nonlinear effects, we followed the standard approach [7,8] with extensions to higher order [9]. We compared the results of these models, as implemented in the `KQUAD` element in `Pelegant` [10,11], with direct integration of particles through a 3D field map generated with OPERA, using `Pelegant`'s `BMXYZ` element. The agreement of the linear matrix elements for a single quadrupole was within 0.01%. In spite of the unusual appearance of the gradient profiles, subsequent rematching of the linear optics succeeded in reducing the changes in the linear optics functions to under 2%, with exact restoration of the tunes. The required changes in magnet excitation were less than 0.6%.

Although the linear optics based on [6] agreed very well with integration through the field map, the nonlinearities showed poor agreement. After some investigation, we concluded that this resulted from the non-Maxwellian character of the 3D field map, which is partly a result of limitations of the magnet code and partly a result of the use of linear interpolation of the field map during integration. Hence, we switched to use of a generalized gradient expansion [12,13], albeit using a non-symplectic integration technique for expediency. (This is available as the `BGGEXP` element in the next release of `elegant/Pelegant`.) Although the generalized gradient expansion (GGE) uses data from the same OPERA simulations, the GGE guarantees that the fields in the interior of the analysis cylinder satisfy Maxwell's equations.

* Work supported by the U.S. Department of Energy, Office of Science, Office of Basic Energy Sciences, under Contract No. DE-AC02-06CH11357.

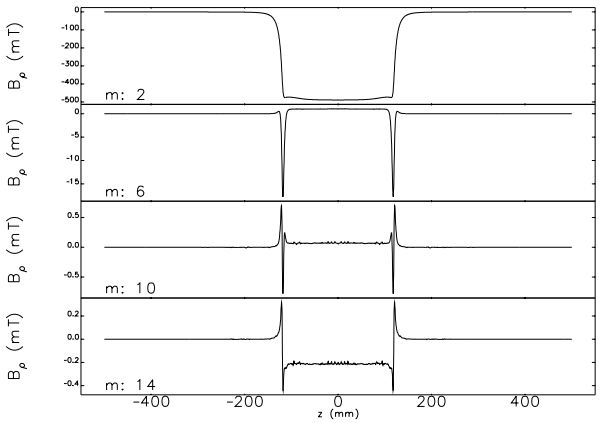

Figure 2: Multipoles of the radial field component at ρ = 10mm for the 98% efficiency case as reconstructed from the GGE.

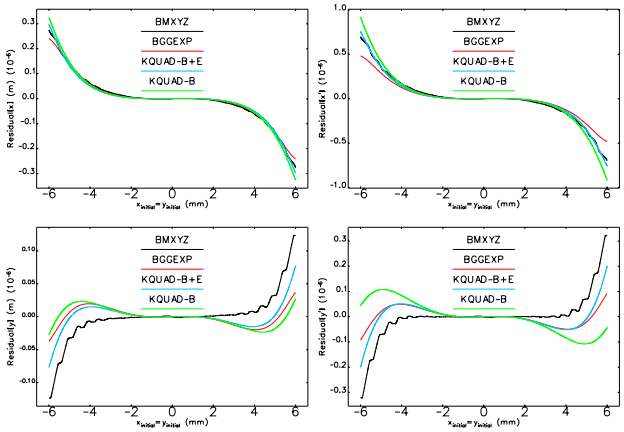

Figure 3: Residuals from linear fit after propagation of a line of particles with initial $x = y$ through a single quadrupole (98% efficiency case) using different methods. "KQUAD-B+E" has edge and body multipoles, whereas "KQUAD-B" uses the uniform body-only multipole model; integrated multipoles are the same in both cases.

Although use of the GGE improved agreement between KQUAD and direct integration, it was still less than ideal. Using the GGE to reconstruct the fields corresponding to various multipoles, as illustrated in Fig. 2, indicated a path forward. Clearly evident are the spikes in the systematic multipoles (12-, 20-, and 28-pole) at the entrace and exit of the magnets. Modeling the effect of these multipoles as a distributed term throughout the body of the quadrupole, as is commonly done, seems suspect. Based on this, we augmented KQUAD to include separate specification of edge and body multipoles. This provided significantly improved agreement with BGGEXP, as illustrated in Figs. 3 and 4.

Based on these results, KQUAD with multipoles separated into body and edge components is being adopted for modeling of APS-U. A symplectically-integrated implementation of BGGEXP is under development, but is expected to be an order of magnitude slower than KQUAD.

Finally, to be conservative, the use of mushroom pole shapes was abandoned. Instead, quadrupole lengths are allowed to vary in order to provide a minimum of 90% efficiency at 10% above the planned operating point.

DIPOLE MODELING

Dipole modeling likewise began with a 3D field map generated with OPERA, in this case, for the M1 dipole. This dipole has 5 segments of gradually decreasing field strength and increasing length. In this case, the use of a GGE is much more involved [14] and has not yet been attempted by us. However, the quality of the field appears in some respects better than for the quadrupoles, judging by the smoothness of the residuals. We once again made use of numerical integration through the 3D field map, this time using the abrat program (distributed with elegant) and the BRAT element in Pelegant. These integrate through bending magnet field maps, with appropriate coordinate transformations at the entrance and exit. A basic test involves tracking a bundle of initially parallel rays with $y = 0$, as shown in Fig.

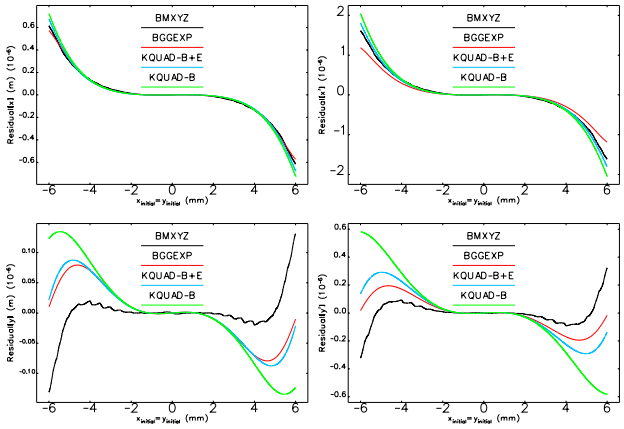

Figure 4: Residuals from linear fit, 67% efficiency case.

5. Inspection of this figure shows that there is a nonlinear variation of the deflecting field at the transitions between the magnet segments. Figure 6 shows residuals of fits to the final slopes, from which we see a clear indication of a sextupole component.

To assess the impact of the linear and nonlinear transport properties of the dipole, we used the analyze_map command in Pelegant to obtain the third-order matrix by tracking through the field map for the M1 diople, using the method outlined in [15]. This involves tracking about 5,000 particles, which takes about 30 seconds on 20 cores. Inserting these into the APS-U lattice gave tune erors of $\Delta\nu_x/\nu_x = 0.019\%$ and $\Delta\nu_y/\nu_y = -0.7\%$, along with corresponding distortions of the lattice functions. These are easily corrected using lattice quadrupoles, giving residual lattice function changes of less than $\sim$ 1% with gradient changes of less than 0.6%.

After lattice correction there are residual chromaticity errors of $\Delta\xi_x = -0.19$ and $\Delta\xi_y = 0.37$ (compared to a target

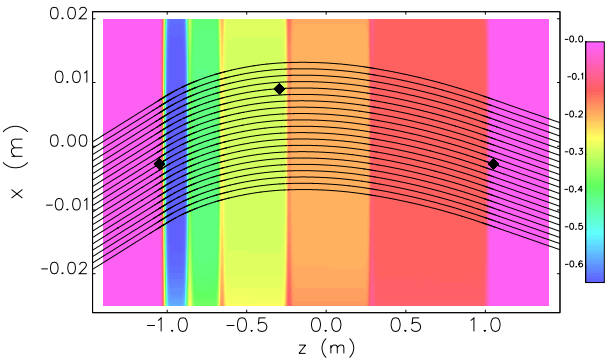

Figure 5: Field map for the M1 dipole, along with `abrat` tracking results for a bundle of initially-parallel rays. The symbols, in order from left to right, are the nominal entrance, vertex, and nominal exit points.

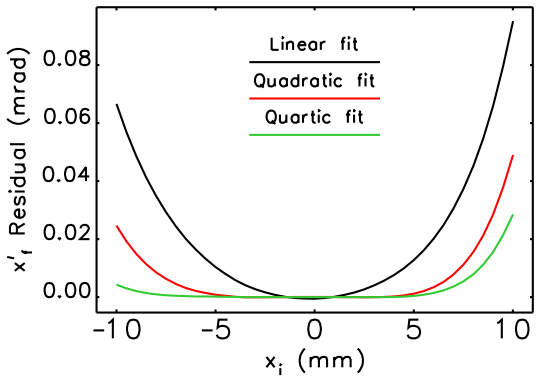

Figure 6: Residuals of fits of various orders to final x' vs initial x for a bundle of parallel rays in the M1 dipole.

chromaticity of 5). Approximating the dipole by its linear map changes these errors to $\Delta\xi_x = 0.06$ and $\Delta\xi_y = 0.43$, which implies that the chromaticity change is partly due to residual lattice changes, and partly due to higher-order terms in the dipole itself. In any case, these are easily corrected with modest adjustments of the sextupoles.

Tracking through the simulated dipole field is a numerically intensive task that is undesirable for use in lattice optimization and evaluations. In addition, the dipole field appears to be well-represented by a small number of low-order multipoles. For these reasons we have begun work to represent the dipole via a "symplectified" Taylor map. The basic idea of a symplectified Taylor map is to first find a Taylor map expression for the element in question to a given order, and then to compute a symplectic approximation of the map that agrees with the Taylor map to that given order. Higher order terms will in general deviate from the actual map, and in fact depend on the way in which the symplectic representation is found.

The first step in finding a symplectic map is to determine the Taylor map approximation for the dipole. For example, we have used the fitting procedure of `analyze_map` described previously to compute its third order matrix. Because the symplectification process is not unique, however, it is important for the initial Taylor map approximation to be (nearly) symplectic up to the order of the Taylor map itself. Unfortunately, we have found that the dipole's third order Taylor map computed using `BRAT` and `analyze_map` is not even approximately symplectic at third order; we believe that this is primarily due to interpolation errors of the magnetic field that do not respect $\nabla \cdot \mathbf{B} = 0$, although numerical errors in the field map and the choice of a non-symplectic integration scheme may also be to blame. Overcoming these difficulties will require a divergence-free representation of the dipole field, which can naturally be found using generalized gradients. We are in the process of extending our previous use of the GGE to include elliptical boundaries [14] which will be able to enclose all relevant trajectories though the entire dipole field; this expansion may also find use in representing APS-U insertion devices.

Once a faithful and divergence-free representation of the magnetic field is found, we expect that `BRAT` tracking will provide a suitable third order map of the dipole. Nevertheless, we also plan to compare these results with fully symplectic tracking based on the implicit midpoint rule, which will allow us to assess the impact of fourth (and higher) order terms. Once we have the Taylor map in had, we must choose our symplectification method. There are many such methods (see, e.g., [16, 17] and references therein), but for expediancy we will first employ the scheme described in Ref. [18]. This method is essentially a practical implementation of previous work that employs the Baker-Campbell-Hausdorff formula to transform the map into a product of monomial maps that in turn have analytic representations [19]. The code implementing the symplectification procedure was freely given by the authors of Ref. [18], so that we can now symplectify a third order Taylor map.

CONCLUSIONS

Progress has been made towards understanding how best to model beam dynamics in quadrupoles and dipoles for the APS upgrade. For quadrupoles, we found that separating the systematic multipoles into edge and body terms provides reasonable agreement with the slower but accurate method of numerically-integrating through reconstructed fields. For dipoles, we assessed effects of the longitudinal gradient dipole field map on linear optics and chromaticity, finding these to be easily compensated. Work continues on developing a symplectic map for such dipoles.

ACKNOWLEDGMENTS

The authors wish to thank M. Venturini (LBNL) for help understanding issues with quadrupole modeling and the use of generalized gradients; A. Jain (ANL) for discussion of the generalized gradient expansion; M. Jaski (ANL) for providing field map data for quadrupoles and dipoles; and Y. Li (BNL) for discussion of symplectic Taylor maps and for sharing his code for map symplectification.

REFERENCES

[1] D. Einfeld et al. *NIM-A*, 335:402 (1993).

[2] M. Borland et al. *Proc. IPAC15*, 1776–1779 (2015).

[3] M. Borland et al. *these proceedings*. WEPOB01.

[4] M. Borland et al. *J Synchrotron Radiation*, 21:912 (2014).

[5] J. Irwin et al. *Proc. of PAC95*, 2376–2378 (1996).

[6] D. Zhou et al. *Proc. of IPAC10*, 4500–4502 (2010).

[7] G. E. Lee-Whiting. *NIM A*, 76 (1969).

[8] E. Forest. *Beam Dynamics: A New Attitude and Framework*. CRC Press (1998).

[9] C. X. Wang. Private communication.

[10] M. Borland. ANL/APS LS-287, Advanced Photon Source (2000).

[11] Y. Wang et al. *AIP Conf Proc*, 877:241 (2006).

[12] M. Venturini. *Lie methods, exact map computation, and the problem of dispersion in space-charge dominated beams*. Ph.D. thesis, University of Maryland (1998).

[13] M. Venturini et al. *NIM A*, 427:387 (1999).

[14] C. E. Mitchell et al. *Phys Rev ST Accel Beams*, 13:06400 (2010).

[15] M. Borland. *A High-Brightness Thermionic Microwave Electron Gun*. Ph.D. thesis, Stanford University (1991). SLAC-402.

[16] A. J. Dragt. *Lie Methods for Nonlinear Dynamics with Applications to Accelerator Physics*. University of Maryland (2009).

[17] E. Forest. *J Phys A: Math Gen*, 17:5321 (2006).

[18] Y. Li et al. A practical approach to extract symplectic transfer maps numerically for arbitrary magnetic elements (2015). ArXiv:1511.00710.

[19] A. Chao. SLAC-PUB-9574, SLAC (2002).